Doxorubicin Encapsulation Investigated by Capillary Electrophoresis with Laser-Induced Fluorescence Detection

Romana Konecna, Hoai Viet Nguyen, Maja Stanisavljevic, Iva Blazkova, Sona Krizkova, Marketa Vaculovicova, Marie Stiborova, et al.

Chromatographia
An International Journal for Rapid Communication in Chromatography, Electrophoresis and Associated Techniques

ISSN 0009-5893
Volume 77
Combined 21-22

Chromatographia (2014) 77:1469-1476
DOI 10.1007/s10337-014-2733-6

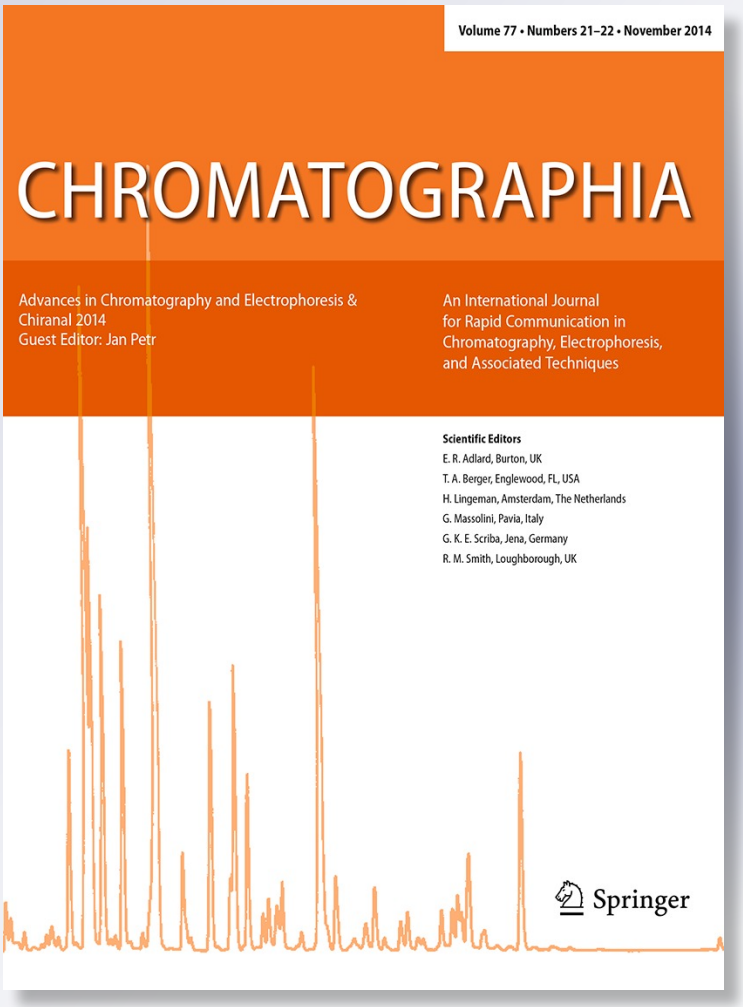

Springer

Chromatographia (2014) 77:1469–1476
DOI 10.1007/s10337-014-2733-6

ORIGINAL

Doxorubicin Encapsulation Investigated by Capillary Electrophoresis with Laser-Induced Fluorescence Detection

Romana Konecna · Hoai Viet Nguyen · Maja Stanisavljevic · Iva Blazkova · Sona Krizkova · Marketa Vaculovicova · Marie Stiborova · Tomas Eckschlager · Ondrej Zitka · Vojtech Adam · Rene Kizek

Received: 18 February 2014 / Revised: 16 May 2014 / Accepted: 24 June 2014 / Published online: 17 August 2014

Abstract Doxorubicin (DOX) belongs to the group of anthracycline antibiotics with very effective anticancer properties. On the other hand, the cardiotoxic effects limit its application over the maximum cumulative dose. To overcome this obstacle, encapsulation of this drug into the protective nanotransporter such as apoferritin is beneficial. In this study, fluorescent behavior of DOX in various solvents was determined by fluorescence spectrometry, demonstrating the fluorescence quenching effect of water, which is often used as a solvent. It was found that by increasing the amount of the organic phase in the DOX solvent the dynamic quenching is significantly suppressed. Ethanol, acetonitrile and dimethyl sulfoxide were tested and the best linearity of the calibration curve was obtained when above 50 % of the solvent was present in the binary mixture with water. Moreover, pH influence on the DOX fluorescence was also observed within the range of 4–10. Two times higher fluorescence intensity was observed at pH 4 compared to pH 10. Further, the DOX behavior in capillary electrophoresis (CE) was investigated. Electrophoretic mobilities (CE) in various pH of the background electrolyte were determined within the range from 16.3 to -13.3×10^{-9} m^{-2} V^{-1} s^{-1}. Finally, CE was also used to monitor the encapsulation of DOX into the cavity of apoferritin as well as the pH-triggered release.

Keywords Capillary electrophoresis · Fluorescence · Drug delivery · Doxorubicin · Apoferritin

Published in the topical collection *Advances in Chromatography and Electrophoresis & Chiranal 2014* with guest editor Jan Petr.

R. Konecna · H. V. Nguyen · M. Stanisavljevic · I. Blazkova · O. Zitka · V. Adam · R. Kizek
Department of Chemistry and Biochemistry, Faculty of Agronomy, Mendel University in Brno, Zemedelska 1, 61300 Brno, Czech Republic

S. Krizkova · M. Vaculovicova · O. Zitka · V. Adam · R. Kizek
Central European Institute of Technology, Brno University of Technology, Technicka 3058/10, 61600 Brno, Czech Republic

M. Stiborova
Department of Biochemistry, Faculty of Science, Charles University, Albertov 2030, 12840 Prague 2, Czech Republic

T. Eckschlager
Department of Paediatric Haematology and Oncology, 2nd Faculty of Medicine, Charles University, and University Hospital Motol, V Uvalu 84, 15006 Prague 5, Czech Republic

R. Kizek (✉)
Central European Institute of Technology and Department of Chemistry and Biochemistry, Mendel University in Brno, Zemedelska 1, 61300 Brno, Czech Republic
e-mail: kizek@sci.muni.cz

Introduction

Anthracyclines belong to the most effective anticancer drugs, whereas doxorubicin (DOX) as one of their main representatives is highly efficient and widely used. This compound was firstly isolated from *Streptomyces peucetius* in 1960s [1]. In spite of the high efficiency and decades of the using, the administration of the drug over the cumulative dose 550 mg/m^2 of body surface area lead to severe side effects including high risk of cardiomyopathy [2, 3], which usually arises the first year after therapy. Nevertheless, cardiac failures can be identified at smaller doses too. This cardiotoxicity is the main force driving the progress towards less toxic formulations enabling also targeted delivery of the drug [4–10].

Due to the optical properties of DOX as well as its biological activity, this molecule is still a target of numerous

investigations [11–13]. The DOX fluorescence in relation to the surrounding conditions such as its concentration, nature of solvent and/or presence of quenchers has been exploited [14]. It is thanks to these fluorescent properties that it is possible to track DOX and its formulations including apoferritin- or liposome-encapsulated forms designed to diminish its toxicity by numerous bioanalytical methods [15]. Besides capillary electrophoresis (CE) also HPLC with fluorescence [16], electrochemical detection [17] and/or mass spectrometric detection [18] has been used. Capillary electrophoresis, in particular, has been utilized for analysis of liposome-encapsulated DOX [19], daunorubicin [20] and/or oxaliplatin [21]. Encapsulation of DOX to nanoparticles preserves the antitumor activity while reducing to risk of cardiotoxicity and increasing distribution of drug to the tumor site. Nowadays, only one commercially available encapsulated DOX is liposome-DOX, called Myocet. The cumulative dose of DOX was increased to 750 mg/m^2 to not reach above-mentioned side effects [22].

In our study, the fluorescent behavior of DOX in the presence of various fluorescence quenchers was investigated followed by capillary electrophoretic study of encapsulation of DOX into the cavity of protein based nanotransporter called apoferritin. The behavior of DOX in CE using various electrolytes differing in pH values was investigated due to the requirement of exploration of DOX release from the apoferritin cage by the pH change.

Experimental Section

Fluorescence Spectrometry

Doxorubicin (5, 10, 20, 30, 40 and 50 μg/mL) was dissolved in water to investigate the behavior depending on concentration. Besides, to explore the influence of organic solvent, DOX (5, 10, 20, 30, 40 and 50 μg/mL) was dissolved in 12.5, 25, 50, 75 and 100 % mixtures of organic solvents (*v*/*v*, ethanol, acetonitrile, and dimethyl sulfoxide) and water. Finally, DOX (5, 10, 20, 30, 40 and 50 μg/mL) was dissolved in buffers of pH ranges 4–10 (acetate pH 4 and 5, phosphate pH 6, 7, 8, borate pH 9, 10). All chemicals were purchased from Sigma Aldrich (USA). Fluorescence intensity was measured at 600 nm after excitation by the light with emission wavelength of 480 nm using the TECAN Infinite 200 PRO microtitration plate reader (Switzerland).

Spectrophotometry

Apoferritin was dissolved in water in concentrations of 0.4, 0.8, 1.6 and 3.2 mg/mL. Absorbance spectra were measured using the TECAN microtitration plate reader Infinite 200 PRO (Switzerland) in the wavelength range 230–600 nm using 50 μL of the sample in the UV transparent 96-well plate. Each absorbance value is an average of 5 measurements.

Preparation of Apoferritin Encapsulated DOX (APODOX)

Various volumes of DOX (2 mg/mL) 25, 50, 75, 100 and 200 μL were filled with water up to 300 μL and mixed with 20 μL of apoferritin (50 mg/mL). The pH 2 was adjusted by HCl to disassemble the apoferritin structure. Subsequently, the pH was adjusted to 7 using NaOH to reassemble the cage. To remove the excess of the DOX, the samples were filtered using Amicon 3K centrifuge filter at 6,000*g* for 15 min.

Capillary Electrophoresis

Apoferritin characterization was performed using CE with UV detection (CE 7100, Agilent Technologies, Germany) and DOX and APODOX were analyzed by CE-LIF (PACE MDQ, Beckman Coulter, USA). In both cases, fused silica capillary with internal diameter of 75 μm and with the total length 64.5 cm (54 cm to detector window) was used. The separation voltage of 20 kV and hydrodynamic injection by 3 psi for 10 s was employed.

Results and Discussion

Study of DOX by Fluorescence Spectrometry

Because of the fact that the fluorescence behavior of DOX (chemical structure shown in inset in Fig. 1a) is one of the main advantages of application of this drug as a model cytostatic drug, this behavior has to be well known and characterized. In our study, solutions of DOX within the concentration range of 5–50 μg/mL were used. It was found that above 50 μg/mL, a significant quenching effect was determined. This quenching is caused by several synergic effects including (a) concentration quenching when the concentration of 50 μg/mL is exceeded and (b) solvent quenching caused by water molecules present in the solution.

Taking into account the fact that solvent influences DOX fluorescence, we studied also the effect of pH. The same concentration range of DOX was prepared with three buffers (acetate, phosphate, and/or borate) covering the pH range 4–10. The fluorescence intensities of DOX in above-mentioned buffers are shown in Fig. 1a. It was found that the fluorescence of DOX was enhanced in acidic pH. The fluorescence of DOX solution with concentration of 50 μg/mL at pH 4 was 2.7-fold higher than at pH 10; however, the

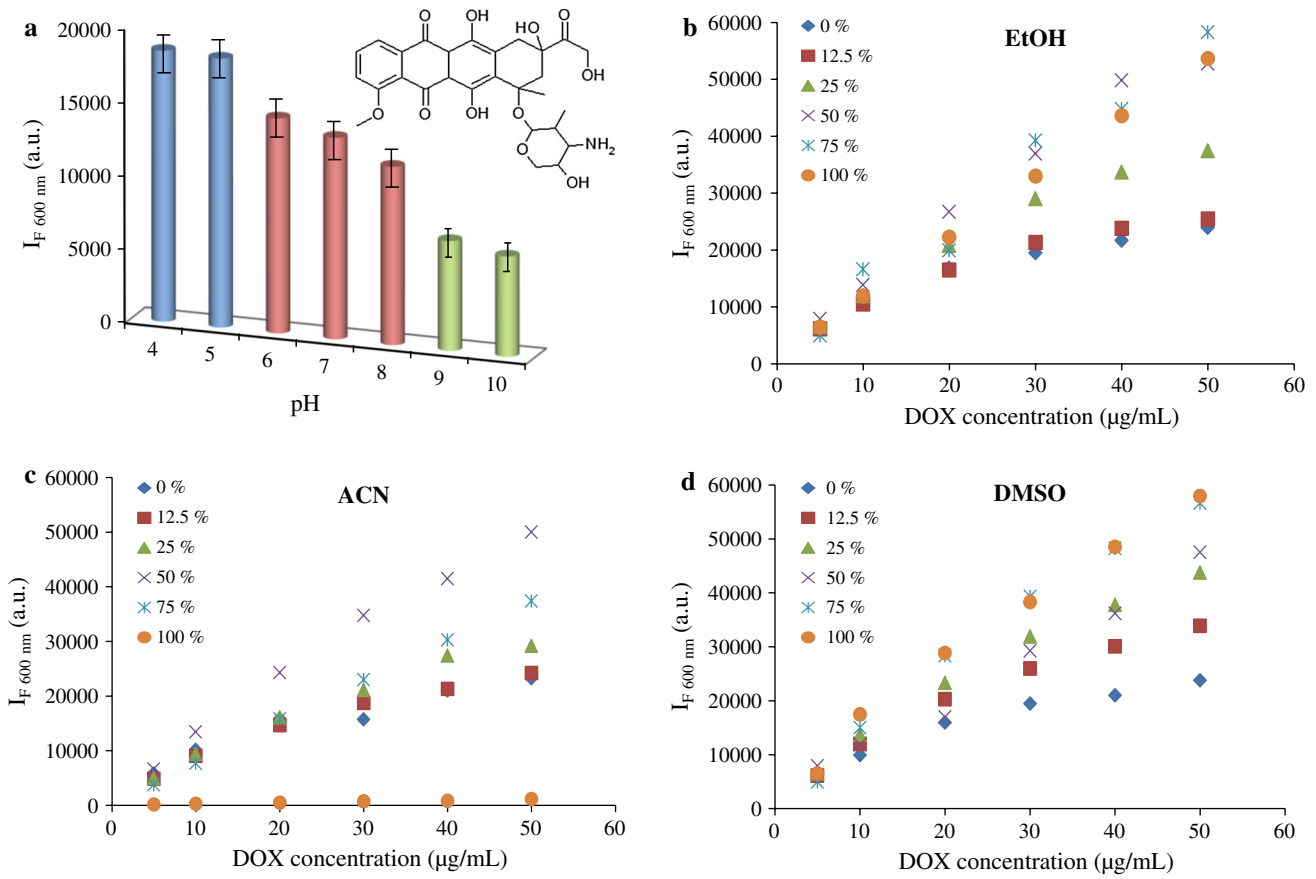

Fig. 1 Characterization of DOX fluorescence measured in various solvents. **a** Dependence of DOX (50 μg/mL) fluorescence intensity on pH of the solvent (*blue* acetate buffer pH 4 and 5, *red* phosphate buffer pH 6, 7 and 8, *green* borate buffer pH 9 and 10). **b**–**d** Dependence of the fluorescence intensity of DOX dissolved in solution containing different percentage of organic solvent 0, 12.5, 25, 50, 75 and 100 % **b** EtOH **c** ACN **d** DMSO. Excitation 480 nm, emission 600 nm

increase in the fluorescence was not linearly dependent on pH. It follows from the results that the nature of the buffer played a role and some proton-exchanging reaction should be taken into the account.

Due to the polar character of water, significant dynamic quenching occurs when water is used as a solvent. To characterize the behavior of DOX in less polar environment, three organic solvents with different physico-chemical properties were used as ethanol, acetonitrile and dimethyl sulphoxide. Binary water mixtures of each solvent were prepared containing 12.5, 25, 50, 75 and 100 % of the organic phase (*v*/*v*). In these mixtures, DOX solutions within concentration range of 5–50 μg/mL were prepared. It follows from the obtained data that the increasing portion of the organic solvent in the mixture leads to the enhancement of the DOX fluorescence. In the other words, the decreasing water portion caused lowering of the quenching effect. If we take a look at the single non-water solvents, the results of EtOH–water mixture used for DOX dissolution are shown in Fig. 1b. The DOX solutions prepared in water exhibit a significant nonlinearity over the selected concentration range (logarithmic trend); however, with the increasing of the organic phase the linearity was significantly improved. Therefore, linear trend line was used for all the curves and the linearity of the calibration curve (coefficient of determination, R^2) was used as a parameter characterizing the solvent effect (Table 1). The increasing linearity of the calibration curve expresses the elimination of water quenching effect. Similarly, it was observed that the slope of each curve increased depending on the increasing organic part. This result highlights the fact that the sensitivity of fluorimetric determination of DOX increases according to the organic phase. Same investigation was carried out using ACN as a solvent (Fig. 1c). The linearity increase depending on ACN percentage was similar to the results obtained in EtOH (Table 1), however, the employment of 75 and 100 % ACN led to the significant decrease in the slope. This fact is caused by diminishing of the sensitivity caused by restricted solubility of DOX under these conditions. Finally, the behavior of DOX in DMSO: water mixtures exhibited the same trend as previous two solvents (Fig. 1d). The linearity as well as the slope of the

Table 1 Summary of regression equations and coefficients of determination for measuring of dependence of peak height on doxorubicin concentration in water mixtures containing various percentages of tested organic solvent

Percentage of organic solvent (*v*/*v*)	EtOH	ACN	DMSO
0	$y = 362.03x + 7{,}338.5$ $R^2 = 0.9208$	$y = 361.71x + 5{,}956.3$ $R^2 = 0.9372$	$y = 374.94x + 6{,}382.3$ $R^2 = 0.9424$
12.5	$y = 427.93x + 6{,}226.3$ $R^2 = 0.9390$	$y = 417.48x + 4{,}676.2$ $R^2 = 0.9621$	$y = 603.83x + 5{,}784.1$ $R^2 = 0.9625$
25	$y = 694.42x + 5{,}310.5$ $R^2 = 0.9692$	$y = 548.99x + 3{,}836.8$ $R^2 = 0.9747$	$y = 813.22x + 5{,}162.9$ $R^2 = 0.9798$
50	$y = 1{,}049.2x + 4{,}240.3$ $R^2 = 0.9792$	$y = 952.64x + 3{,}822.2$ $R^2 = 0.9903$	$y = 876.06x + 2{,}312.7$ $R^2 = 0.988$
75	$y = 1{,}133.8x + 1{,}353.2$ $R^2 = 0.9726$	$y = 746.4x + 369.64$ $R^2 = 0.9993$	$y = 1{,}032.4x + 6{,}539.2$ $R^2 = 0.9902$
100	$y = 1{,}051.2x + 1{,}322.4$ $R^2 = 0.9999$	$y = 20.959x + 51.562$ $R^2 = 0.9886$	$y = 1{,}005.6x + 8{,}029.4$ $R^2 = 0.9989$

calibration curve increased with the portion of the organic phase. The results are summarized in Table 1. From the obtained data it can be concluded that all three organic solvents are able to diminish the dynamic quenching of DOX fluorescence caused by the presence of water molecules. In the case of ACN the determination is affected only by the limited solubility of DOX. From the results it also follows that DMSO supports the DOX fluorescence the most because the signal of 50 µg/mL DOX increased 2.2-fold in EtOH and 2.4-fold in DMSO.

Capillary Electrophoretic Study of DOX

The behavior of the analyte in various environments is one of the key aspects that have to be considered prior to analysis by capillary electrophoresis. Compared with the stationary fluorimetric measurements, analysis by separation methods such as capillary electrophoresis with laser-induced fluorescence detection, may provide valuable information on the presence of various components, contaminations or even analyte species in the studied solution. Due to the complex structure of DOX and due to the presence of several functional groups, DOX may occur as a cation, anion, zwitterion and/or neutral molecule depending on the environment. Structure of anionic and cationic form is shown in Fig. 2a. To determine the form of DOX, simple method using CE can be utilized. As expected, the fluorescence signal of the obtained peaks is linearly proportional to the concentration of DOX. The peak height plotted over the concentration of DOX exhibits the linear tendency with regression equation $y = 6.9652x - 0.31$ and determination coefficient $R^2 = 0.9981$.

To determine the ionic form of DOX and its pI, phosphate buffer with pH 3, 4, 6, 8, 10, or 11 was used as a separation electrolyte and coumarin 334 was employed as an EOF marker. The obtained electropherograms are shown in Fig. 2b. pH as low as 3 caused very slow EOF and therefore only DOX peak was obtained, however, the increasing pH above this value, peaks of both DOX and coumarin 334 were detected. DOX migrated as a cation (before the EOF marker) in the pH up to 10. When the pH was increased to 11, the peak of DOX occurred after the EOF marker, which confirmed the anionic form of DOX. As expected, based on previous fluorimetric experiments, the peak height of DOX decreased with the increasing pH (Fig. 2c left). From the migration times, the electrophoretic mobilities were calculated (Fig. 2c right). It clearly follows from the results obtained that the electrophoretic mobilities change over the range from 16.3×10^{-9} to -13.2×10^{-9} $m^2\ V^{-1}\ s^{-1}$.

For the following experiments, it was also necessary to evaluate the behavior of DOX when the pH of the BGE and sample (DOX) zone does not match. As it was expected, the sample stacking occurred due to the dynamic pH junction phenomenon. To demonstrate this fact, the pH of BGE was kept constant (6) and the pH of sample zone was 4, 6, and/or 8. In the case of sample zone pH 4, 2-fold increase in DOX peak height was observed. The signal of DOX measured in the presence of solution of pH 8 was negligible (when matching the BGE and sample zone pH); however, using the described non-matching conditions, the detection of DOX was possible (Fig. 2d left). Because the optimization of sample stacking was not the primary aim of this study, no further improvement in this direction was carried out. Calculating the electrophoretic mobility confirmed that the behavior of the analyte under used condition is independent on the pH of the sample zone and it migrated with the mobility given by the BGE (13.3×10^{-9} $m^2\ V^{-1}\ s^{-1}$) (Fig. 2d right).

CE Characterization of Apoferritin

Apoferritin is a naturally occurring protein serving as a reservoir of iron ions in the living organisms. This protein has a ball-like structure with 12 nm in diameter containing a hollow cavity of 8 nm in size. This protein is capable of pH-dependent disassembling and reassembling allowing encapsulation of desired molecules in the cavity. This process is utilized for application of apoferritin as a nanocarrier of targeted molecule [8, 10, 23]. In this study the

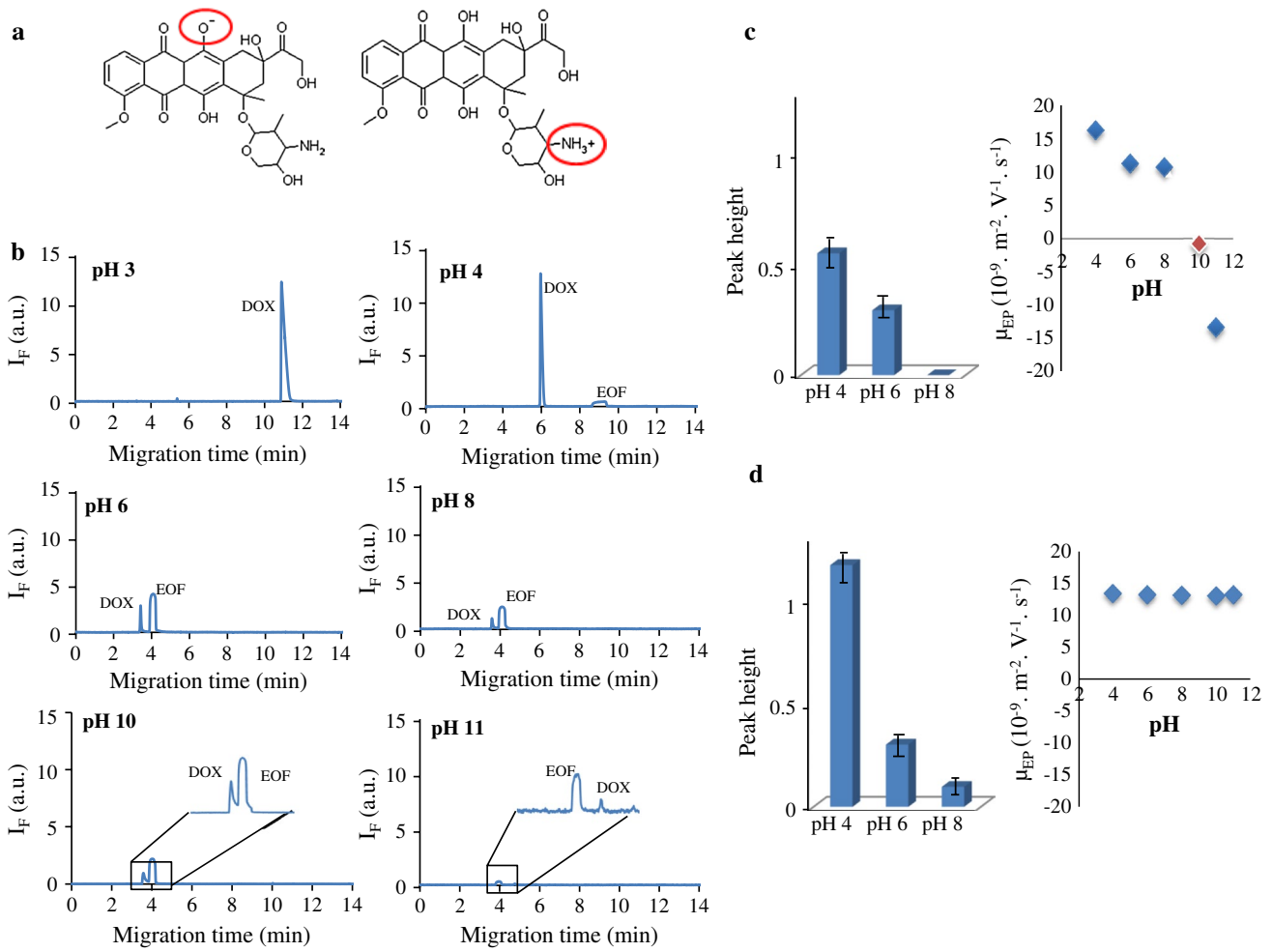

Fig. 2 **a** Structure of DOX in anionic and cationic form. **b** CE-LIF of DOX with pH matching to BGE pH, DOX concentration 0.5 μg/mL, CE conditions: capillary 75 μm, 64.5/54 cm; voltage +20 kV; injection 3 psi, 10 s; BGE 10 mM sodium phosphate pH 3, 4, 6, 8, 10 or 11. **c** *Left* DOX peak heights obtained when BGE pH matched sample zone pH (BGE 10 mM phosphate buffer pH 4, 6 and 8), *right* electrophoretic mobilities of DOX under conditions matching the pH of BGE and DOX zone. **d** *Left* DOX peak heights obtained for BGE pH mismatching the sample zone pH (BGE 10 mM phosphate buffer pH 6, sample zone pH 4, 6 and 8), *right* electrophoretic mobilities of DOX for pH of BGE mismatching the DOX zone

apoferritin was utilized to encapsulate DOX and the process was monitored by CE.

At first, CE-UV analysis of apoferritin was carried out determining the possibility of CE analysis using the phosphate buffer as it is shown in Fig. 3. The pI of apoferritin is 4.4 and therefore under used CE conditions, the protein was in an anionic form and migrated after the EOF (Fig. 3a). It was observed that the dependence of peak height on concentration was linear with coefficient of determination $R^2 = 0.9956$ and the equation $y = 1.405x + 1.7503$. The spectrophotometric analysis of apoferritin of different concentration is shown in the inset in Fig. 3a Due to the beneficial apoferritin properties enabling the pH-triggered disassembling of its structure this protein has perfect qualities for encapsulation of drug such as DOX. To exploit these properties, it was necessary to observe the behavior of apoferritin under various pH conditions by CE. As it is shown in Fig. 3b the peak height of the protein decreased with its pH. On the other hand, the influence of the pH on the migration time was not so significant. The summary of the peak heights as well as migration times depending on the pH is shown in the inset in Fig. 3b.

APODOX

In this study, apoferritin was used as a transporter of doxorubicin and CE-LIF was tested as a method of the monitoring of the encapsulation. The pH-directed apoferritin disassembling and reassembling as well as DOX encapsulation is schematically shown in Fig. 4a. To determine the encapsulation of DOX into the apoferritin cavity, a set of APODOX samples was prepared using a different amount of

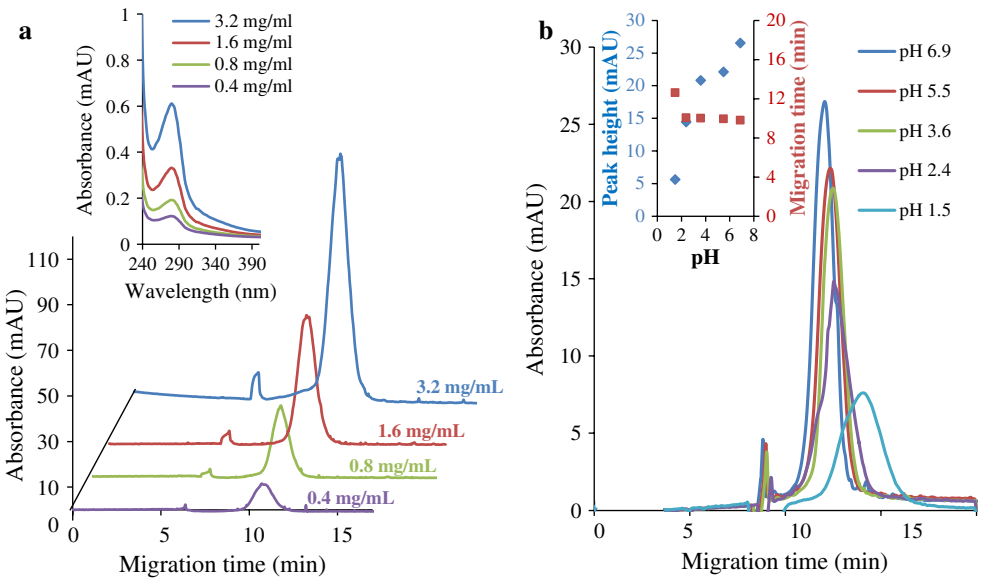

Fig. 3 **a** CE-UV of apoferritin (detection 214 nm, capillary ID 75 µm, length 54/62.5, buffer 10 mM sodium phosphate pH 6, injection 3 psi 10 s, voltage +20 kV); *inset* absorption spectra of apoferritin; **b** CE-UV of apoferritin in different pH, conditions same as in Fig. 3a *inset* concentration dependence of the apoferritin peak height and migration time

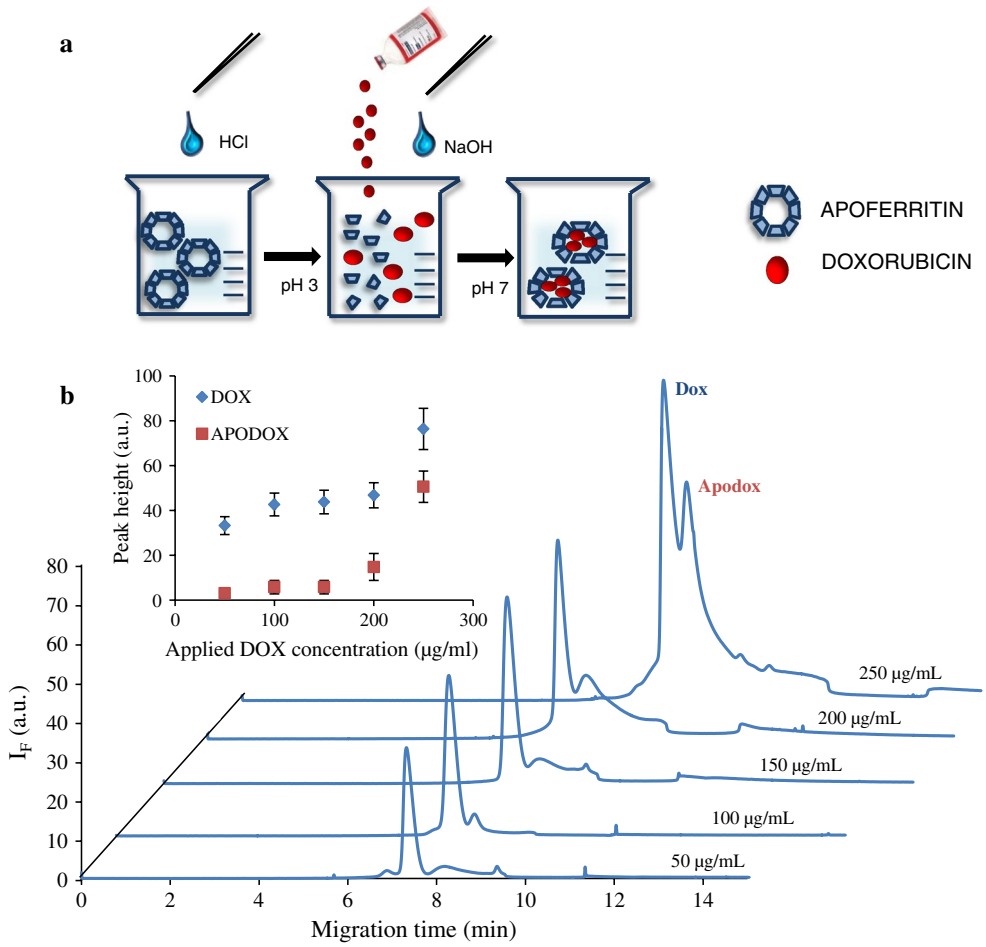

Fig. 4 **a** Scheme of encapsulation of DOX into the apoferritin and its pH-regulated release. **b** CE-LIF of Apodox formed by the increasing applied concentration of DOX (BGE: 10 mM phosphate, pH 6, capillary ID 75 µm, 64.5/54 cm, voltage +20 kV, injection 3 psi, 10 s, detection ex 488 nm/em 600 nm); *inset* dependence of peak height on DOX concentration

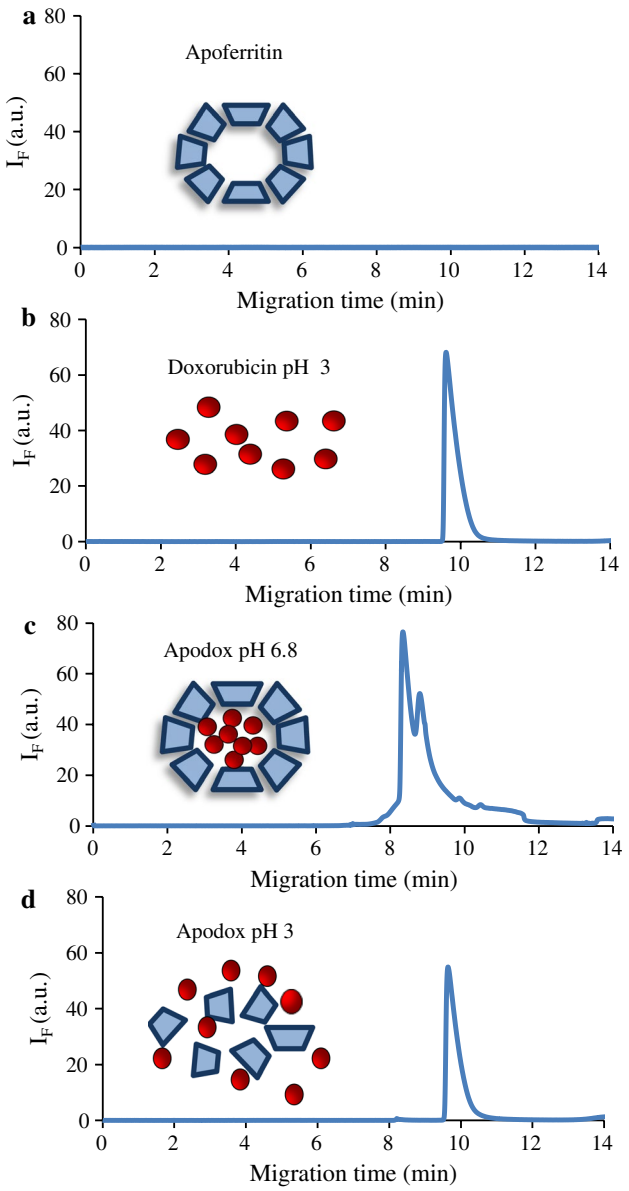

Fig. 5 **a** CE-LIF of apoferritin (1.6 mg/mL), *inset* schematics of apoferritin structure. **b** CE-LIF of DOX (3 μg/mL) at pH 3, *inset* schematics of DOX molecules. **c** CE-LIF of APODOX at pH 6.8, *inset* scheme of DOX encapsulated in apoferritin. **d** CE-LIF of APODOX at pH 2, *inset* schematic APODOX disassembling by low pH; (BGE: 10 mM phosphate, pH 6, capillary ID 7 5 μm, 64.5/54 cm, voltage +20 kV, injection 3 psi, 10 s, detection ex 488 nm/em 600 nm)

applied DOX (50–250 μg/mL). Subsequently, the samples were analyzed by CE-LIF and typical electropherograms are shown in Fig. 4b. The two major signals were identified. The first peak represents DOX molecule adsorbed on the apoferritin surface and released by electric field. The second peak labeled "APODOX" is attributed to DOX encapsulated into the cavity of apoferritin. As shown in the inset in Fig. 4b, the increase in the applied DOX concentration led to the increase in both signals. Similarly to gel electrophoresis the highest intensities of two main peaks were detected in the sample with applied 250 μg/mL of DOX.

The pH-triggered release was demonstrated by electrophoretic analysis (Fig. 5). Due to the fact that apoferritin does not exhibit any fluorescence, there is no signal present in the CE-LIF analysis of apoferritin (Fig. 5a). Subsequently, DOX solution with pH adjusted to 3 was analyzed providing a peak with migration time of 10 min. (Fig. 5b). This was compared to the electropherogram of APODOX (Fig. 5c) with pH of 6.8 as well as APODOX with pH decreased to 3 (Fig. 5d). Comparing these three electropherograms, it can be concluded that lowering the pH of APODOX to 3 led to the occurring of a single peak matching the migration time to the DOX at the same conditions. Based on these results, the release of the DOX was proven.

Conclusion

The fluorescent properties of DOX are strongly dependent on the environment and the increasing pH as well as the presence of water causes the fluorescence quenching. Using CE, the electrophoretic mobility of DOX as well as the pI was calculated. Finally, CE-LIF has been proven to be an effective tool for monitoring of the encapsulation into the apoferritin cavity as well as controlled pH-triggered release.

Acknowledgments The financial support from GA CR CYTORES P301/10/0356 is highly acknowledged.

Conflict of interest Authors declare no conflict of interest.

References

1. Weiss RB (1992) Semin Oncol 19:670–686
2. Zagotto G, Gatto B, Moro S, Sissi C, Palumbo M (2001) J Chromatogr B 764:161–171
3. Singal PK, Iliskovic N (1998) N Engl J Med 339:900–905
4. Zhen ZP, Tang W, Guo CL, Chen HM, Lin X, Liu G, Fei BW, Chen XY, Xu BQ, Xie J (2013) ACS Nano 7:6988–6996
5. Meng LJ, Zhang XK, Lu QH, Fei ZF, Dyson PJ (2012) Biomaterials 33:1689–1698
6. Tacar O, Sriamornsak P, Dass CR (2013) J Pharm Pharmacol 65:157–170
7. Wang YG, Wei XL, Zhang CL, Zhang FY, Liang W (2010) Ther Del 1:273–287
8. Blazkova I, Nguyen HV, Dostalova S, Kopel P, Stanisavljevic M, Vaculovicova M, Stiborova M, Eckschlager T, Kizek R, Adam V (2013) Int J Mol Sci 14:13391–13402
9. Drbohlavova J, Chomoucka J, Adam V, Ryvolova M, Eckschlager T, Hubalek J, Kizek R (2013) Curr Drug Metab 14:547–564
10. Tmejova K, Hynek D, Kopel P, Dostalova S, Smerkova K, Stanisavljevic M, Nguyen HV, Nejdl L, Vaculovicova M, Krizkova S, Kizek R, Adam V (2013) Int J Electrochem Sci 8: 12658–12671
11. Baran TM, Foster TH (2013) Laser Surg Med 45:542–550

12. Li DA, Zhang YT, Yu M, Guo J, Chaudhary D, Wang CC (2013) Biomaterials 34:7913–7922
13. Schenone AV, Culzoni MJ, Campiglia AD, Goicoechea HC (2013) Anal Bioanal Chem 405:8515–8523
14. Karukstis KK, Thompson EHZ, Whiles JA, Rosenfeld RJ (1998) Biophys Chem 73:249–263
15. Perez-Ruiz T, Martinez-Lozano C, Sanz A, Bravo E (2001) Electrophoresis 22:134–138
16. Ali RMM, Reimold I, Fricker G, Haefeli WE, Burhenne J (2009) Br J Clin Pharmacol 68:34
17. Riley CM, Runyan AK, Grahampole J (1987) Anal Lett 20:97–116
18. Mazuel C, Grove J, Gerin G, Keenan KP (2003) J Pharm Biomed Anal 33:1093–1102
19. Kim HS, Wainer IW (2010) J Pharm Biomed Anal 52:372–376
20. Griese N, Blaschke G, Boos J, Hempel G (2002) J Chromatogr A 979:379–388
21. Franzen U, Nguyen T, Vermehren C, Gammelgaard B, Ostergaard J (2011) J Pharm Biomed Anal 55:16–22
22. Mross K, Niemann B, Massing U, Drevs J, Unger C, Bhamra R, Swenson C (2004) Cancer Chemother Pharmacol 54:514–524
23. Dospivova D, Hynek D, Kopel P, Bezdekova A, Sochor J, Krizkova S, Adam V, Trnkova L, Hubalek J, Babula P, Provaznik I, Vrba R, Kizek R (2012) Int J Electrochem Sci 7:6378–6395